MEASUREMENT OF AXIAL STRESS DISTRIBUTIONS IN FRP-CONFINED CONCRETE COLUMNS USING TEKSCAN PRESSURE SENSORS

J.G. Teng[1], J.J. Zeng[2] and J.F. Chen[3,4]

[1] Department of Civil and Environmental Engineering, The Hong Kong Polytechnic University, Hong Kong, China. Email: cejgteng@polyu.edu.hk (Corresponding Author)

[2] Department of Civil and Environmental Engineering, The Hong Kong Polytechnic University, Hong Kong, China. Email: bobbyzjj@gmail.com

[3] School of Civil and Transportation Engineering, Guangdong University of Technology, Guangzhou, China

[4] School of Planning, Architecture and Civil Engineering, Queen's University Belfast, Belfast, UK. Email: J.Chen@qub.ac.uk

Keywords: FRP, Confinement, Rectangular column, Axial stress distribution, Pressure sensor, Strengthening

ABSTRACT

Strengthening of reinforced concrete (RC) columns through the provision of lateral confinement using fiber-reinforced polymer (FRP) jackets is now a widely accepted technique. While the behavior of concrete uniformly confined with FRP, as is found in FRP-confined circular concrete columns under concentric compression, is now well understood, there is much less understanding of the behavior of concrete non-uniformly confined with FRP (e.g. FRP-confined rectangular columns under axial compression). A major difficulty with existing studies on concrete columns under non-uniform FRP confinement lies in the lack of knowledge of precise stress distributions in such columns, and as a result, direct verification in terms of internal stress distributions of analytical/numerical models for FRP-confined concrete in these columns has been impossible. Against this background, the present paper presents the first ever study on the measurement of axial stress distributions in FRP-confined rectangular columns under concentric compression using a new pressure mapping technique. The measurement technique is first introduced, and the procedure for obtaining axial stresses in FRP-confined column is then explained. A comparison between the experimental results and the predictions of an advanced finite element model is next given, which provides mutual verification of the two methods.

1 INTRODUCTION

Strengthening of reinforced concrete (RC) columns through the provision of lateral confinement using fiber-reinforced polymer (FRP) jackets is now a widely accepted technique. Consequently, the behavior of FRP-confined concrete in both circular and rectangular columns has been studied by many researchers. The behavior of concrete uniformly confined with FRP, as is found in FRP-confined circular concrete columns under concentric compression, is now well understood, and many stress-strain models have resulted from these studies for such FRP-confined concrete. On the contrary, research the behavior of concrete non-uniformly confined with FRP (e.g. FRP-confined rectangular concrete columns under concentric compression and FRP-confined circular concrete columns under eccentric compression) has been much more limited. A major difficulty with existing research on concrete columns under non-uniform FRP confinement has been the lack of accurate measurement of stress distributions in such columns due to the limitation of measurement techniques, and as a result, direct verification in terms of internal stress distributions of analytical/numerical models for FRP-confined concrete in these columns has been impossible. In particular, the existing analytical modeling work on the stress-strain behavior of concrete in FRP-confined rectangular columns has relied heavily on the assumption of an "effective-confinement area" (e.g. [1, 2]) that originated from Mander's *et al.* [3] work on steel-confined rectangular columns, but the reliability of this assumption has never been

experimentally proven.

Against the above background, the present paper presents the first ever study on the measurement of axial stress distributions in FRP-confined rectangular columns under concentric compression using a new pressure mapping technique. The experimental results provide valuable clarifications of axial stress distributions in FRP-confined rectangular concrete columns.

2 PRESSURE MEASUREMENT USING THE I-SCAN SYSTEM

2.1 I-Scan pressure mapping system

The I-Scan pressure mapping system is a matrix-based tactile pressure sensing system available from Tekscan Inc. The technology was initially developed at MIT's Artificial Intelligence Laboratory by Hillis [4]. The system includes data acquisition electronics, sensors, and software. These pressure mapping sensors are usually very thin (i.e., around 0.1 mm), with each consisting of a unique piezoresistive material sandwiched between two pieces of flexible polyester with printed silver conductors on each piece (Figure 1). Due to the small thickness, these sensors have a broad range of applications [5]. The silver conductors are designed into rows and columns which intersect to form sensels. When a normal force is exerted on a sensel, the electrical resistance in the piezoresistive material changes in inverse proportion to the force [6]. Pressure measurement can thus be linked to the measurement of changes in the electrical resistance. Through the use of appropriate electronics and software, the measurement results can be interpreted and recorded by a PC.

Pressure mapping sensor 5101 [6], which is suitable for general applications, was selected based on the requirements of the present study. The sensor consists of 44 rows and 44 columns of conductive stripes within an area of 110×110 mm^2, with the center-to-center spacing between stripes being 2.5 mm. The pressure rating was 34.475 MPa, which can be adjusted using by a factor of 7 to 1/3 (i.e., capable of measuring a maximum pressure of about 241 MPa) [6].

2.2 Equilibration, conditioning and calibration of the sensor

For the sensor to provide reliable results, it also needs to go through equilibration, conditioning and calibration before use. Equilibration involves the application of a uniform pressure on the entire active area of the sensor [7]. The I-scan software then determines a gain factor for each sensel such that its digital output (DO) is equal to the average DO of all loaded sensels. That is, the equilibrium process normalizes all sensels to compensate for differences in sensitivity between sensels due to manufacturing or repeated use. For a new sensor, equilibration has been conducted in the factory. For an old sensor, equilibration can be conducted to extend the lifespan of the sensor. However, equilibration is not an easy process and user attempts to equilibrate the sensor needs to be done with great care [7]. Equilibration was not done in the present study as all the sensors were used at most twice in the present study.

Conditioning, involving loading the sensor several times to a level at or above the anticipated test load, is needed to reduce the magnitude of drift in sensor readings and improve repeatability. In the present study, appropriate conditioning was done before each test by loading the sensor in the as-test condition several times to an average axial stress equals to 1.3 times the compressive strength of unconfined concrete.

Calibration is the process of correlating the digital output from the sensels with the applied load. The applied load must be precisely known and correctly entered into the software. In this study, the single point calibration option [5] was adopted and the calibration pressure was maintained for one minute or until the pressure appeared to have stabilized [8]. It is worth noting that calibration should be performed on the same test specimen right before each test to avoid unexpected pressure discrepancy caused by different contact surfaces [9] and the reading drift [7]. Although the texture of the surface of concrete is inhomogeneous and calibration does not guarantee the correctness of local pressure values, calibration at each load level is nacessary to ensure the accuracy of total axial load, otherwise the difference between these two readings can be up to 24 % [9]. In the present study, the axial force from both the machince reading and the pressure film (integrated value of stresses from sensels) were monitored at each load level to examine the load drift; it was found that the desprepancy between the loading machine and

the pressure film values was within 2 % for each of the load steps.

2.3 Use of the I-scan prsesure mapping system in civil engineering

The I-scan pressure mapping system has been used in a number of civil engineering applications (e.g. [10-11]). These applications indicate that the I-scan system is likely to be capable of providing detailed internal stress distributions in concrete structures although no previous study has attempted such measurements. Such stress measurements, as mentioned earlier, are highly valuable for understanding the confinement mechanics and providing verification data for finite element models of FRP-confined concrete columns.

3 MEASUREMENT OF AXIAL STRESS DISTRIBUTION

3.1 Experimental programme and material properties

The authors have recently undertaken an experimental study in which the axial stress distributions in FRP-confined square concrete columns were measured using the I-scan pressure mapping system. The column heigth L, section width b, section depth h, section aspect ratio h/b, corner radius and FRP thickness of test specimens are listed in Table 1.These specimens were designed to cover the three key factors that affect the axial stress distribution [1]: section aspect ratio, corner radius and thickness of FRP jacket (Table 1). The columns were confined with CFRP jackets formed via a wet layup process, with all the fibers aligned in the hoop direction. Based on FRP flat coupon tests [12], the tensile elastic modulus and tensile strength of the CFRP were 246.3 GPa and 3993.8 MPa, respectively. The properties of concrete (strength f'_{co} and stain at peak stress ε_{co} of unconfined concrete) from 6 standard 150 mm cylinder tests are given in Table 1.

Table 1 Specimen details

No.	Notation	L	b	h	h/b	Corner radius	t	f'_{co}	ε_{co}
1	S-F2r25	300	150	150	1	25	0.334	42.5	0.0024
2	S-F1r50	300	150	150	1	50	0.167	39.2	0.0025
3	S-F2r50	300	150	150	1	50	0.334	42.5	0.0024
4	**R125F2r25**	**332**	**133**	**166**	**1.25**	**25**	**0.334**	**42.5**	**0.0024**
5	R150F2r25	368	122	184	1.5	25	0.334	42.5	0.0024
6	R125F2r50	332	133	166	1.25	50	0.334	42.5	0.0024
7	R150F2r50	368	122	184	1.5	50	0.334	42.5	0.0024

The detailed results of all these specimens can be found elsewhere [13]. Here, only the results from one of the columns, namely specimen R125F2r25, are presented to examine the capability and accuracy of the I-scan pressure mapping system.

3.2 Instrumentation

In the present experimental study, the main objective was to measure the axial stress distribution in FRP-confined rectangular concrete columns under concentric compression. To achieve this objective, a column specimen was cast as two half columns so that the pressure sensor could be placed between them at the mid-height of the whole column (Figure 2). To protect the thin, flexible senor from possible delamination due to transverse shear stresses [8], the sensor was placed between two Teflon sheets.

It should also be noted that the sensor was not large enough to cover the whole section of the column specimen (larger sensors were not available to the authors). As a result, only a quarter of the section was covered by the sensor while the other three quarters of the section were leveled using a polyester sheet having the same thickness as the pressure film. The chosen quarter of the section was covered by 33×27 sensels, with the outer sides of the edge stripes coinciding with the two axes of symmetry (Figure 3). The load acting on the sensor was assumed to be a quarter of the total load acting on the column (Figure 3). The validity of this assumption was checked by monitoring the readings of two full-height linear variable differential transformers (LVDTs) on two opposite sides of

the column as well as the four surface axial strain gauges at the four mid-width locations respectively during the loading test. The strains in the FRP jacket on the column were measured by strain gauges installed on the jacket surface at the following two levels: 1) 20 mm below the mid height (level 1-1 shown in Figure 2), and 2) 20 mm above the mid height (level 2-2). It was intended that the strain readings at these two levels would be compared to identify possible differences.

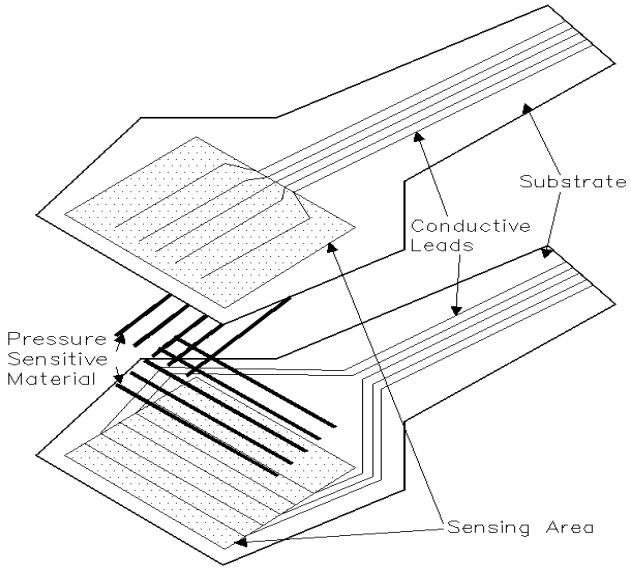

Figure 1 Pressure sensor details

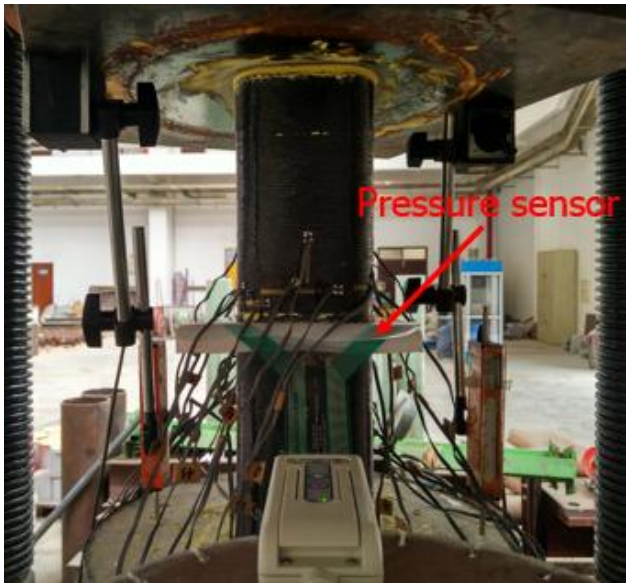

Figure 2 Test set-up

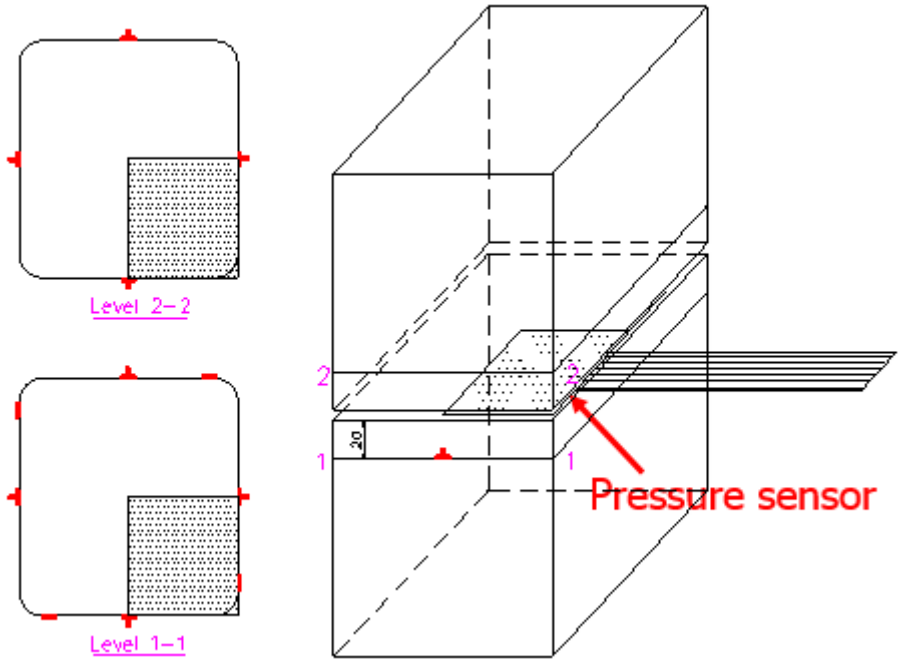

Figure 3 Strain gauges and pressure sensor positions

3.3 Test procedure

The test was performed in displacement control at the rate of 0.24 mm per minute. Loading was paused for 120 seconds for the calibration of the pressure sensor and recording at each target load level. The test was terminated when one of the following conditions was reached: a) the applied average axial pressure reached around 1.3 times the unconfined concrete strength, and b) the maximum hoop strain of the FRP jacked reached 9000 με in order to avoid the rupture of the FRP jacket, which would likely damage the pressure sensor.

4 EXPERIMENTAL RESULTS AND FINITE ELEMENT SIMULATION

4.1 Experimental axial stress distributions

Due to space limitation, only the axial stress distribution from specimen R125F2r25 is examined in this paper. Specimen R125F2r25, like all other CFRP-confined rectangular columns of the present study [13], had a monotonically ascending axial stress-strain response. No FRP rupture was experienced during the test.

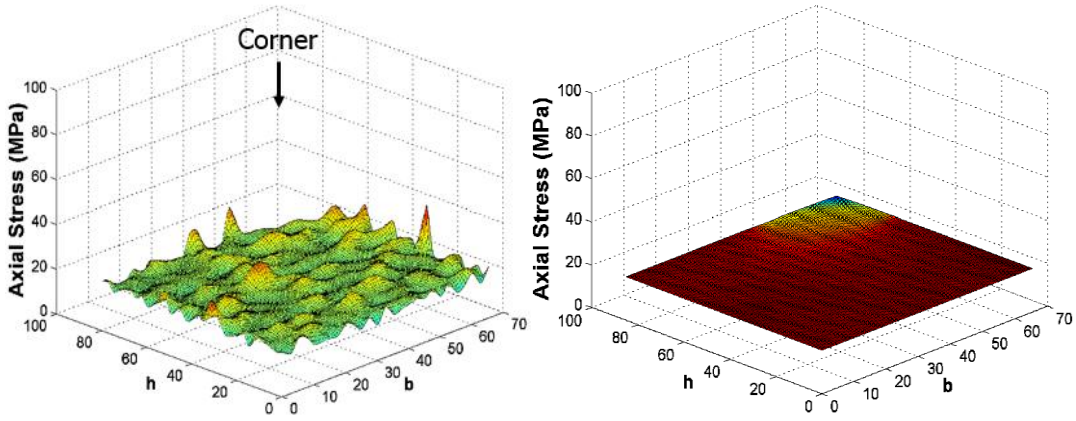

(a) $\sigma_{ca} \approx 0.5 \cdot f_{co}^{'}$ (Test and FE)

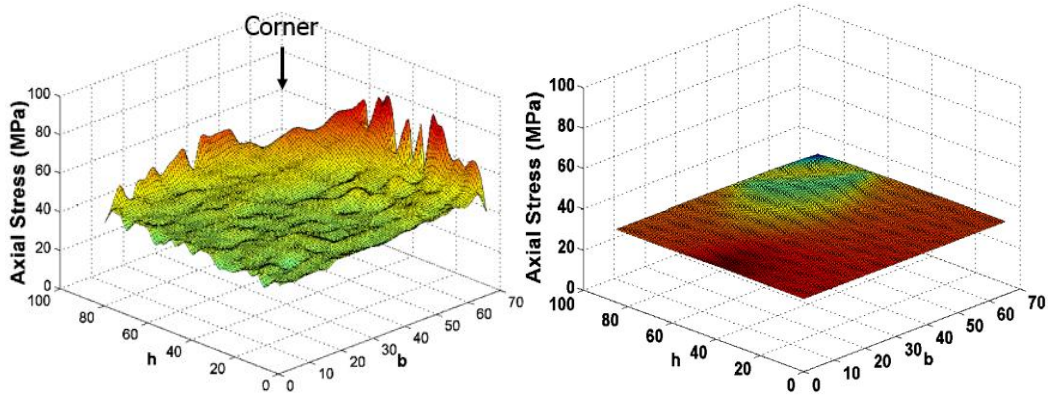

(b) $\sigma_{ca} \approx 1.0 \cdot f_{co}^{'}$ (Test and FE)

Figure 4. Axial stress distribution: experimental results versus FE predictions

The axial stress distributions measured at several average stress levels in Specimen R125F2r25 are presented in Figure 4. It should be noted that these stress levels refer to the sectional average axial stress, σ_{ca}, and are given in terms of the unconfined concrete strength $f_{co}^{'}$ from standard circular cylinder tests. Figure 4 shows that the axial stress distribution is overall flat over the cross-section during the early stage of the test, although significant local fluctuations exist. At stress levels exceeding the unconfined concrete strength, axial stress concentrations in the corner region are obvious. The local fluctuations of axial stresses are over the whole section, which can be attributed to a number of factors, the most obvious of which is the inhomogeneity of the concrete material. For

example, it is not hard to imagine that the coarse aggregate has a great effect on local pressure values over the section.

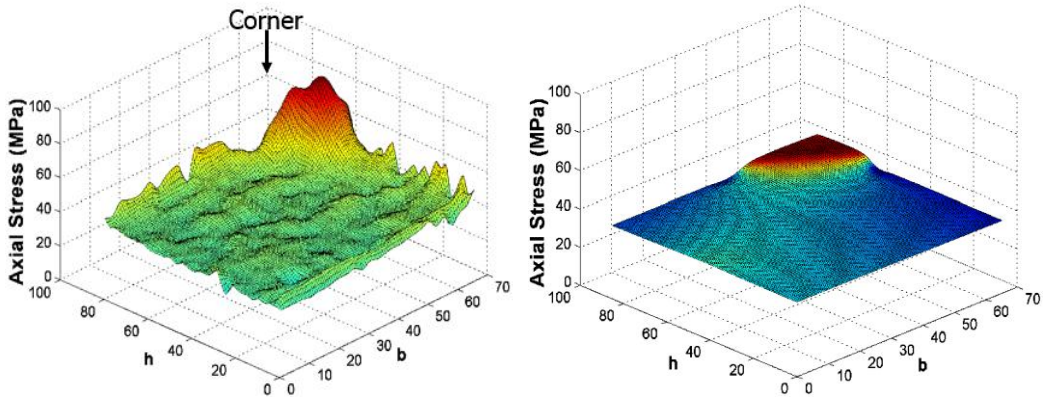

(c) $\sigma_{ca} \approx 1.1 \cdot f_{co}^{'}$ (Test and FE)

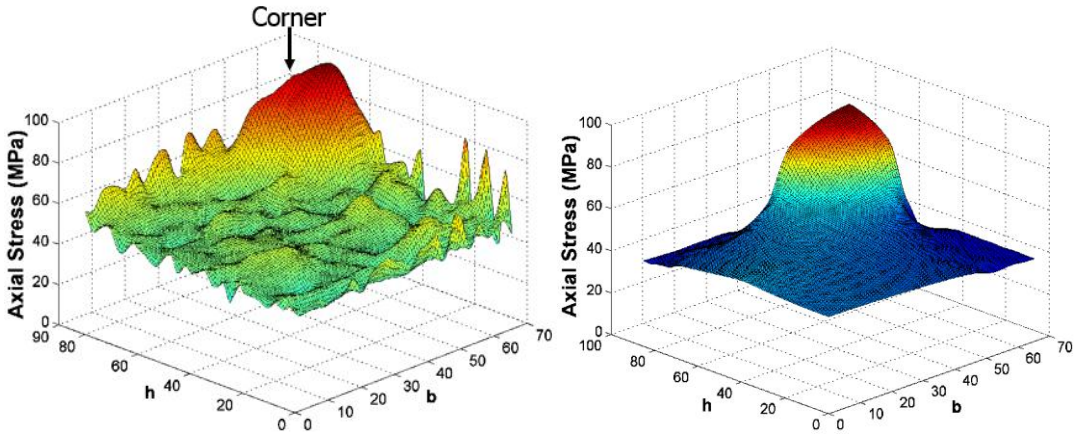

(d) $\sigma_{ca} \approx 1.3 \cdot f_{co}^{'}$ (Test and FE)

Figure 4. Axial stress distribution: experimental results versus FE predictions

4.2 Finite element modelling

A finite element simulation of specimen R125F2r25 was undertaken to obtain results for comparison with the measured axial stresses in the specimen. A slice model was used in the finite element simulation as was done by Yu et al. [14]. The plastic-damage model proposed by Yu et al. [14] and subsequently modified by Teng et al. [15], which was implemented into ABAQUS via the Concrete Damaged Plasticity Model (CDPM) option, was used as the constitutive model for concrete. The concrete core was modeled using solid elements while the FRP jacket was modelled using shell elements.

4.3 Comparison between experimental and finite element results

The predicted axial stress distributions at different stress levels are given in Figure 4. The overall trend of the experimental axial stress distribution is seen to be in reasonably close agreement with that from FE analysis, especially when significant confinement has been mobilized (e.g. when the average axial stress is at 1.3 times $f_{co}^{'}$). For more detailed comparisons, the axial stresses from both approaches along three selected paths at an average stress of 1.3 times $f_{co}^{'}$ are presented in Figure 5, where the horizontal coordinate, x, has its origin at the column centre. These paths were selected as they were expected to show large stress gradients. The experimental values were from the sensels nearest to the designated paths (i.e., the shaded sensels in Figure 5). It can be seen that the stress distributions from the two approaches are in satisfactory agreement given the complexity of the problem; the experimental results oscillate around the FE results due to local fluctuations. These comparisons provide clear evidence for the first time that the finite element method can provide

reasonably close predictions of axial stress distributions in FRP-confined concrete in rectangular columns.

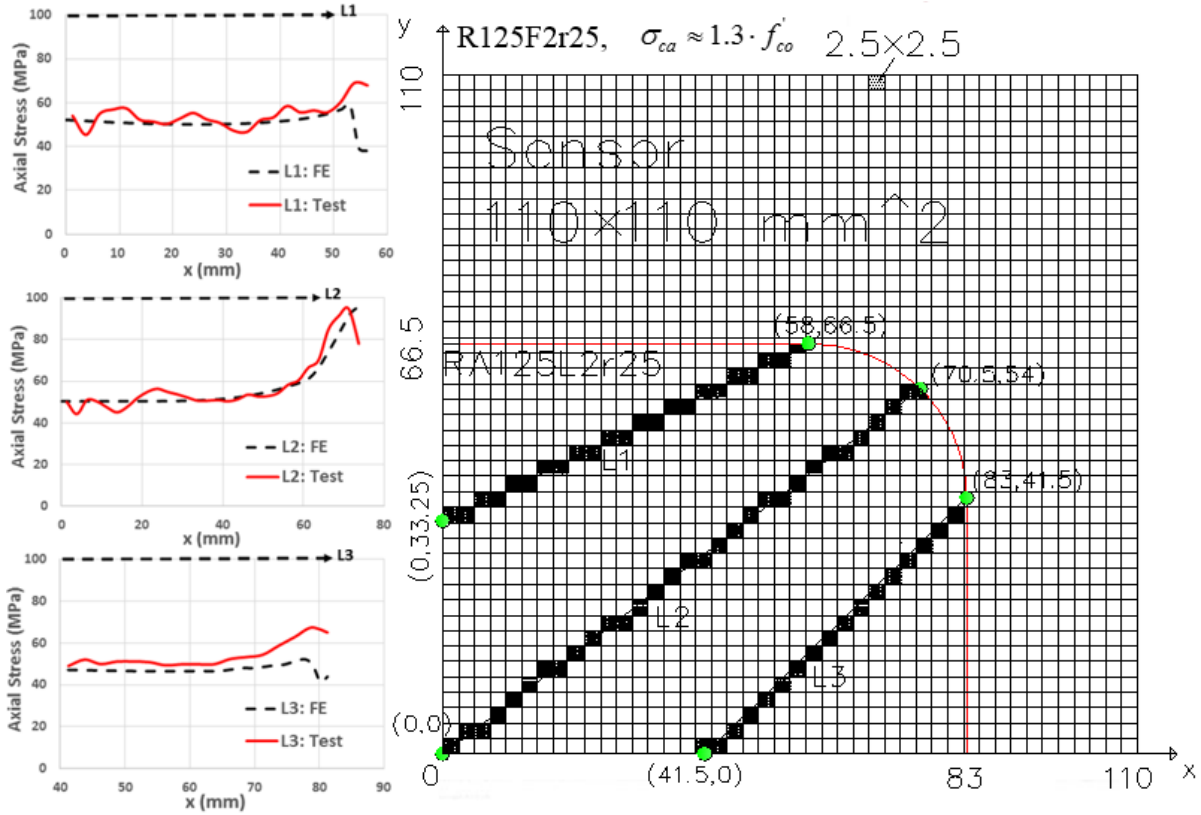

Figure 5. Axial stress variations along selected paths: experimental results versus FE predictions

5 CONCLUSIONS

This paper has briefly presented a study on the measurement of axial stress distributions in FRP-confined rectangular concrete columns using a novel pressure mapping system, the I-scan system [6]. The experimental procedure has been described in some detail, and the results from one of the column specimens have been presented and compared with predictions from an advanced finite element model. Based on the results and discussions presented in the paper, the following conclusions can be drawn:

1. The I-Scan pressure mapping system is capable of providing detailed measurements of internal stresses in FRP-confined concrete columns, and can thus be used in future studies on the confinement mechanics of FRP-confined concrete and on other problems where such measurements are important;
2. Local stress fluctuations were found in the measured axial stresses and can be attributed to the inhomogeneity of concrete; these fluctuations remained almost constant as the loading increased.
3. The test results revealed clearly that that axial stress was uniform over the cross-section (except for the local fluctuations) at the beginning of the test when the stress level was low but became obviously concentrated in the corner region when the average axial stress exceeded its unconfined concrete strength.
4. Comparisons between experimental results and FE predictions showed clearly that the FE model proposed by Yu et al. [14] is capable of producing close predictions of the axial stress distribution.

ACKNOWLEDGEMENTS

The authors are grateful for the financial support received from the National Basic Research Program (i.e. 973 Program) (Project No.: 2012CB026200) of China, the Hong Kong Research Grants Council (Project No.: PolyU 152153/14E) and Guangdong University of Technology, China (Project No.: 112418032).

REFERENCES

[1] L. Lam, J.G. Teng. Design-oriented stress-strain model for FRP-confined concrete in rectangular columns, Journal of Reinforced Plastics and Composites, 2003, 22:1149-1186.

[2] K.G. Megalooikonomou, K.D. Kim, G. Monti. Stress-strain model for FRP-confined rectangular RC sections via an incremental procedure, Proceedings of Asia-Pacific Conference on FRP in Structures (APFIS 2007), Hong Kong, China, 2007, 155-160.

[3] J.B. Mander, M.J. Priestley, R. Park. Theoretical stress-strain model for confined concrete, Journal of Structural Engineering, ASCE, 1988, 114(8):1804-1826.

[4] W.D. Hillis. Active touch sensing, Artificial Intelligence Laboratory Memo 629, Massachusetts Institute of Technology, Cambridge, MA, USA, 1981.

[5] Tekscan. I-Scan User Manual, Tekscan Inc., USA, 2013.

[6] Tekscan. I-Scan Product Selection Guide, Tekscan Inc., USA, 2015.

[7] Tekscan. Tekscan I-Scan Equilibration and Calibration Practical Suggestions, Tekscan Inc., USA, 2003.

[8] M.C. Palmer, T.D. O'Rourke, N.A. Olson, T. Abdoun, D. Ha, M.J. O'Rourke. Tactile pressure sensors for soil-structure interaction assessment, Journal of Geotechnical and Geoenvironmental Engineering, ASCE, 2009, 135(11):1638-1645.

[9] J.M. Brimacombe, D.R. Wilson, A.J. Hodgson, K.T.C. Ho, C. Anglin. Effect of calibration method on Tekscan sensor accuracy, Journal of Biomechanical Engineering, 2009, 131:034503.

[10] J.C. Stith. Railroad Track Pressure Measurements at the Rail/Tie Plate Interface using Tekscan Sensors, Master's Thesis, University of Kentucky, USA, 2005.

[11] S.G. Paikowshy, C.J. Palmer, L.E. Rolwes. The use of tactile sensor technology for measuring soil stress distribution, Proceedings of Geocongress, Atlanta, USA, 2006.

[12] ASTM-D3039. Standard Test Method for Tensile Properties of Plymer Matrix Composite Materials, American Society for Testing and Materials, West Conshohocken, USA, 1995.

[13] J.G. Teng, J.J. Zeng, J.F. Chen. Axial stress distributions in FRP-confined concrete columns: measurement using novel Tekscan pressure sensors, 2015, in preparation.

[14] T. Yu, J.G. Teng, Y.L. Wong, S.L. Dong. Finite element modeling of confined concrete-II: Plastic-damage model, Engineering Structures, 2010, 32(3):680-691.

[15] J.G. Teng, Q.G. Xiao, T. Yu, L. Lam. Three-dimensional finite element analysis of reinforced concrete columns with FRP and/or steel confinement, Engineering Structures, 2015, 97:15-28.